

Precise measurement on the binding energy of hypertriton from the nuclear emulsion data using analysis with machine learning

A. Kasagi^{a,b}, E. Liu^{a,c,d}, M. Nakagawa^a, H. Ekawa^a, J. Yoshida^{a,e}, W. Dou^{a,f}, A. Muneem^{a,g}, K. Nakazawa^{b,h}, C. Rappoldⁱ, N. Saito^a, T. R. Saito^{a,j,k}, M. Taki^l, Y. K. Tanaka^a, and H. Wang^a

^a*High Energy Nuclear Physics Laboratory, Cluster for Pioneering Research, RIKEN, 2-1 Hirosawa, Wako, Saitama 351-0198, Japan*

^b*Graduate School of Engineering, Gifu University, 1-1 Yanagido, Gifu 501-1193, Japan*

^c*Institute of Modern Physics, Chinese Academy of Sciences, 509 Nanchang Road, Lanzhou, Gansu Province, 730000, China.*

^d*School of Nuclear Science and Technology, University of Chinese Academy of Sciences, No.19(A) Yuquan Road, Shijingshan District, Beijing, 100049, China.*

^e*Department of physics, Tohoku University, Aramaki, Aoba-ku, Sendai 980-8578, Japan.*

^f*Department of Physics, Saitama University, Saitama, 338-8570, Japan.*

^g*Faculty of Engineering Sciences, Ghulam Ishaq Khan Institute of Engineering Sciences and Technology, Topi, 23640, KP, Pakistan*

^h*Faculty of Education, Gifu University, 1-1 Yanagido, Gifu 501-1193, Japan.*

ⁱ*Instituto de Estructura de la Materia, CSIC, Madrid, Spain.*

^j*GSI Helmholtz Centre for Heavy Ion Research, Planckstrasse 1, D-64291 Darmstadt, Germany.*

^k*School of Nuclear Science and Technology, Lanzhou University, 222 South Tianshui Road, Lanzhou, Gansu Province, 730000, China.*

^l*Graduate School of Artificial Intelligence and Science, Rikkyo University, 3-34-1 Nishi Ikebukuro, Toshima-ku, Tokyo 171-8501, Japan.*

Received 15 January 2022; accepted 11 February 2022

A machine learning model has been developed to search for events of production and decay of a hypertriton in nuclear emulsion data, which is used for measuring the binding energy of the hypertriton at the best precision. The developed model employs an established technique for object detection and is trained with surrogate images generated by Monte Carlo simulations and image transfer techniques. The first hypertriton event has already been detected with the developed method only with 10^{-4} of the total emulsion data. It implies that a sufficient number of hypertriton events will soon be detected for the precise measurement of the hypertriton binding energy.

Keywords: Hypernucleus; hypertriton; binding energy; nuclear emulsion; machine learning.

DOI: <https://doi.org/10.31349/SuplRevMexFis.3.0308122>

1. Introduction

Hypernuclei have been studied for approximately seven decades to investigate the baryonic interactions under the flavored SU(3) symmetry. The first hypernucleus was observed in nuclear emulsions, which were irradiated by high-energy cosmic rays [1]. After the discovery, the binding energies of the Λ -hyperon, *i.e.*, the Λ separation energy, were studied with the nuclear emulsion technique and K^- meson beams at CERN [2,3]. Recently, experimental techniques with real-time particle counters using secondary meson- and primary electron-beams as well as heavy ion beams have been established and are employed for studying the binding energies, structure, and lifetimes of hypernuclei [4–6]. However, the emulsion technique still has a great advantage in measuring the binding energy of light hypernuclei at the best precision.

A nuclear emulsion is a special photographic film, which is able to detect the tracks of charged particles. When a

charged particle passes through an emulsion layer, its three-dimensional trajectory is recorded and can be visualized after chemical developments. Thanks to the small size of silver halide crystal, approximately 200 nm, a spatial resolution of better than a micrometer for reconstructing tracks of charged particles can be achieved by observing clusters of grains with an optical microscope. For hypernuclear studies, tracks of charged particles associated with the decay of hypernuclei can be observed precisely by analyzing nuclear emulsion images. An invariant mass of hypernuclei is deduced by measuring kinetic energies and momentum of these charged particles; thus, the Λ -binding energy of hypernuclei is determined. However, since all events are accumulated and superimposed without time information, a huge number of tracks unrelated to the production and decay of hypernuclei are also recorded. Therefore, a hypernuclear event must be dug out from the huge background. Searches of hypernuclear events in the nuclear emulsion have manually been performed

by visual inspections with an optical microscope, which takes a vast amount of time and labor load. Nuclear emulsions were used for precise measurements of hypernuclear binding energies until the 1970's, accordingly; the information of hypernuclear binding energies is not updated for several light hypernuclei.

Recently, the binding energy of light hypernuclei has attracted renewed interest. This topic was triggered by the investigation of hypertritons by experiments using heavy ion beams. Hypertriton is the lightest hypernucleus composed of a deuteron core and a Λ hyperon. The binding energy between the Λ and the deuteron was measured by the emulsion technique, and the reported value is 130 ± 50 keV [3]. This value is generally used as an input value in theoretical calculations for hypernuclei; therefore, the hypertriton is the benchmark in the field of hypernuclear physics. Furthermore, this result suggests that the Λ is weakly bound to the deuteron core, and the lifetime of hypertriton has been considered to be close to the lifetime of free- Λ , 263 ps [7]. Recently, the experiments using heavy ions such as the HypHI, the STAR, and the ALICE collaborations show that the derived lifetimes of hypertriton, $183_{-32}^{+42}(\text{stat.}) \pm 37(\text{syst.})$ ps [8], $182_{-45}^{+89}(\text{stat.}) \pm 27(\text{syst.})$ ps [9] and $181_{-39}^{+54}(\text{stat.}) \pm 33(\text{syst.})$ ps [10], respectively, are shorter than the lifetime of free- Λ . However, it is hard to reproduce these short lifetimes by theoretical calculations due to the observed small binding energy of the hypertriton from 1970's [3]. The STAR and ALICE updated their measurements on the hypertriton lifetime, and the reported values are $142_{-21}^{+24}(\text{stat.}) \pm 29(\text{syst.})$ ps [11, 12] and $242_{-38}^{+34}(\text{stat.}) \pm 17(\text{syst.})$ ps [13], respectively. These values deviated, and their accuracy is not sufficient to determine whether the hypertriton lifetime is shorter than or equal to the lifetime of Λ .

The binding energy of hypertriton is essential for the lifetime puzzle because theoretical calculations point out a correlation between the binding energy and the lifetime [14]. In 2020, the STAR collaboration derived the binding energy of hypertriton [15]. The reported value $410 \pm 110(\text{stat.}) \pm 100(\text{syst.})$ keV is much larger than the formerly known value; however, the accuracy of this result is insufficient to draw a definite conclusion. Even though the hypertriton is a benchmark of hypernuclear physics, its nature is still unclear, both in terms of binding energy and lifetime.

For the lifetime of hypertriton, efforts will be made at several facilities [17–20] to improve the accuracy. For the binding energy, in addition to the scheduled projects at STAR [21] and ALICE [22], nuclear emulsion provides a great opportunity to reach high accuracy. It can be achieved by analyzing the recent nuclear emulsion data taken by the J-PARC E07 experiment [23]. This paper describes a new method for analyzing the existing E07 nuclear emulsion data combined with the modern machine learning technique [18].

2. Analysis method for nuclear emulsion data with Machine learning

Detection of hypertriton events is performed in the nuclear emulsion irradiated by K^- beams in the E07 experiment at J-PARC [23], aiming at searching for double-strangeness hypernuclei. It was proposed that approximately a hundred events associated with double-strangeness hypernuclei can be observed by using the so-called hybrid method [23]. In this method, a Ξ^- hyperon produced by the (K^- , K^+) reaction is identified and tracked by other real-time detectors when the outgoing K^+ is detected. The position where a Ξ^- hyperon enters a stack of emulsion layers is estimated according to measured tracks of Ξ^- hyperon by the other real-time detectors, and the Ξ^- hyperon track is followed until it is stopped and captured by a nucleus in the emulsion [24]. At the captured point, the Ξ^- hyperon may convert into two Λ s by interaction with a proton of the nucleus near the stopped point and may produce a double-strangeness hypernucleus.

Further visual inspections with an optical microscope are performed around the stop position of Ξ^- hyperons and have detected double-strangeness hypernuclear events [25–27]. In this experiment, hypertritons should also be produced in the E07 emulsion, and the tracks associated with their production and decay should have been recorded. However, most hypertritons were produced by direct interactions of K^- beams and nuclei in the emulsion without incoming Ξ^- hyperons and outgoing K^+ tracks. Thus, the detection of hypertriton was so hard with the hybrid method, and no information was obtained for the production of hypertriton. Therefore, taking data from the entire volume of nuclear emulsion sheets so-called Overall Scanning method [28, 29], is necessary to detect events of hypertritons.

The data acquired by scanning is a grayscale image as shown in panel a) of Fig. 1. Each black line and dot correspond to charged particle tracks, and the track density is approximately $10^6/\text{cm}^2$. Events associated with the decay

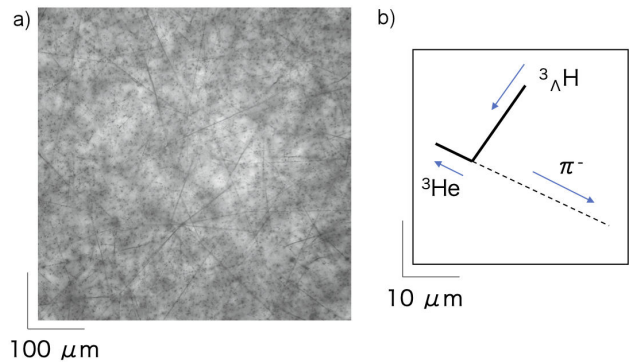


FIGURE 1. a) A micrograph of one of the nuclear emulsion sheets used in the E07 experiment. In this micrograph, many tracks are shown as black lines and dots that correspond to the traces of charged particles penetrating the emulsion. b) A schematic diagram of the two-body decay of the hypertriton at rest.

of hypertriton are needed to be detected from images with such a high density of charged particle tracks. In the present work, we are interested in digging out an event of hypertriton which decays into a two-body final-state, namely, ${}^3\text{He} + \pi^-$, because the length of the π^- track is uniquely defined by the Q-value. The length of π^- track from the two-body decay of hypertriton is approximately 28 mm, and this length is unique and significantly different from the 42 mm the length of π^- track emitted from the similar two-body decay of ${}^4_{\Lambda}\text{H}$, ${}^4_{\Lambda}\text{H} \rightarrow {}^4\text{He} + \pi^-$. When we detect an event of two-body decays of hypernuclei illustrated in the right panel b) of Fig. 1, the length of π^- tracks will be measured by optical microscopes and, therefore, events associated with hypertritons will be uniquely identified.

Developments of a detector for such a T-shaped is needed to detect events of hypertritons. However, a former approach using analytical filters such as line detection [29] was not successful in hypernuclear detection because the shape of the hypertriton decay event is too simple. In the former trial, a huge amount of events were selected as candidates that needed to be sorted out by human visual inspection. The total image data size of all emulsion sheets and the number of events detected by the analytical filters were estimated to be 140 PB and approximately 10^{10} , respectively, which would require over 560 years to analyze all the emulsion sheets. Furthermore, the ratio of the number of tracks associated with hypertriton to the total number of tracks recorded is estimated to be only 10^{-8} . Due to such a small signal-to-noise ratio, the hypertriton has never been detected in the data of the E07 experiment.

Employing machine learning techniques should make significant contributions for detecting hypertriton events in the E07 nuclear emulsion data since these techniques have shown a potential ability for image recognition. A feasibility study to analyze nuclear emulsion data using machine learning was performed with one of the most commonly used convolutional neural networks (CNN) [30,31] prior to the present work, and real images of events selected by the analytical filters and human visual inspections. α -decay events, which are tracks of the decay chain of radioisotopes such as uranium- and thorium-series in the emulsion, were used for the training, validation, and testing of the model. The performance of the developed model was improved by a factor of seven compared to the conventional method, as discussed in the paper [32].

In the present work, a machine learning-based detector of hypertriton events is to be developed with machine learning techniques. Optimizing of a machine learning model requires training data; however, no hypertriton event had been detected in the E07 nuclear emulsion, it was not possible to use real events. Therefore, Monte Carlo simulations were employed to generate data for the production and decay of the hypertriton in the emulsion. These Monte Carlo simulations provide three-dimensional information of the tracks of each particle by using the Geant4 [34]. Panel a) of Fig. 2 shows the tracks of α -decay events in the emulsion sheet generated

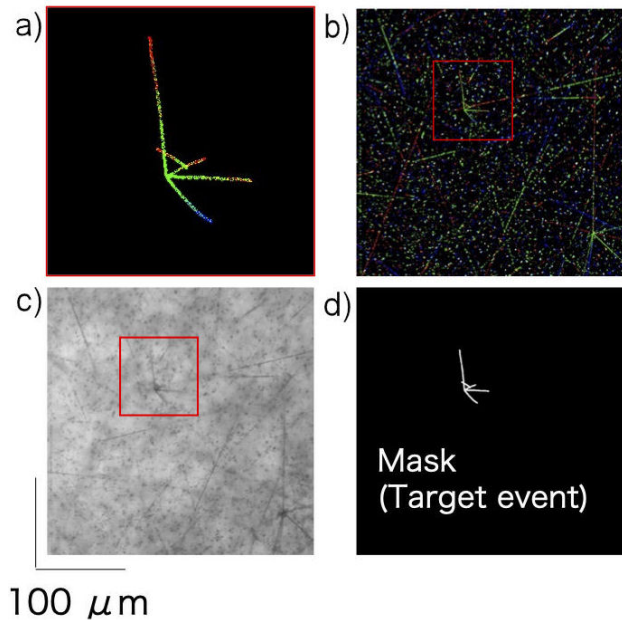


FIGURE 2. a) Tracks of an α -decay generated by Geant4. The green color represents the track within the depth of field of the microscope, and the color change corresponds to the difference in coordinates in the depth direction. b) Color line segment image generated by mixing the simulated events with the background image taken from a real emulsion sheet. The area with a red frame represents the event in panel a). c) The image converted to a microscope image by the model of GAN. d) An example of mask information for the event generated by the simulation.

by the simulation. The color shows the difference of the coordinates in the depth direction to reproduce the defocusing of an optical microscope. Panel b) shows the color image made by mixing simulated α -decay and background image taken randomly from the real emulsion data. Although the image produced by the above procedure reproduces the track information in the emulsion, the image style is different from the real microscope image. One of the machine learning networks, generative adversarial networks (GAN) [35,36], overcomes this difficulty by converting the style of images. The model was trained by pairing microscopic images of the original emulsion with line segment images produced by image processing. The developed model was able to convert each image style to the other. Panel c) shows a surrogate image, including an α -decay event in the emulsion.

An object detection model based on Mask R-CNN [33], a network for detecting the location and shape of target objects in images, was developed with these surrogate images. For the training of the model for object detection, mask information that corresponds to the location and shape of the detection target is required. These mask information are usually created by humans through a time-consuming annotation-work, limiting the amount of training data available for object detection tasks with machine learning. On the other hand, it is easy to obtain the mask information of events generated with Monte Carlo simulations. Therefore, a large amount of

training data enable without annotation work. Panel d) shows an example of mask information for the training data.

The performance of the object detection model was evaluated with the real α -decay events. A visual inspection of a certain region revealed approximately 100 α -decay events. The developed model was applied to search for the α -decay event from images acquired in the same area. The detection efficiency and signal-to-noise ratio of the candidate events selected by the model are approximately 80% and 20%, respectively, which is a twice improvement in detection efficiency and a 20 times improvement in signal-to-noise ratio compared to the performance of the analytical filters [29] for the same data-set.

3. Application for Hypertriton search

The developed method has been employed to search for the hypertriton events. Ten thousands hypertriton events for developing the machine learning model were also generated by Monte Carlo simulations and GAN techniques. The model for hypertriton detection was developed with these surrogate images and was applied to search for hypertriton events from real emulsion data sample. The developed model has improved the signal-to-noise ratio in hypernuclear search from 10^{-8} to 4×10^{-4} , 10^4 times better, and has decreased a load

of human visual inspection significantly. The first hypertriton event has already been detected only with 10^{-4} of the total emulsion data sample of the E07 experiment. Panels a) and b) of Fig. 3 show the raw image of a certain scanned emulsion area in which a hypertriton of interest exits and the detected hypertriton event, respectively. Panel c) shows the overall view of the first detected event, the detail of which is discussed in Ref. [18]. The measured length of the π^- track is 28.80 ± 0.01 mm, and this event was uniquely identified as the two-body decay of hypertriton.

This discovery has guaranteed that the present work will provide precise information on the binding energy of hypernuclei decaying to two-charged particles, including the hypertriton. The binding energy is determined by the invariant mass, which is calculated for each event by measuring the track length of particles from the hypernuclear decay with a proper emulsion density calibration by using accumulated α -decay events near the hypertriton events of interest [37]. The estimated statistical accuracy is approximately ± 500 keV per event, and the systematic uncertainty of the binding energy measurement for hypertriton can be reached to ± 30 keV, as evaluated in Ref [38].

The measured value of the ${}^4_{\Lambda}\text{H}$ binding energy can be used for checking the quality of the developed method in the present work since the binding energy of ${}^4_{\Lambda}\text{H}$ was already measured with reasonable precision by the A1 collaboration at MAMI-C [39].

4. Summary and prospect

We have performed a search for hypertriton events using machine learning techniques for precise measurement of binding energy using a nuclear emulsion. The detector for hypertriton event with a technique for object detection has been trained with surrogate images of emulsion generated by Monte Carlo simulation and GAN techniques. Multiple hypertriton events have already been detected with the emulsion data sample of the E07 experiment. It shows that a large number of hypertriton events will be detected with more data samples, and the binding energy of hypertriton will be derived shortly.

The present work is a milestone for a new step in studying hypernuclei with the emulsion. The searches for other light single- Λ hypernuclei and double-strangeness hypernuclei will be performed to determine their binding energies. In addition, this method is unique from former emulsion experiments in that it directly detects the decay event of hypernuclei. It allows us to simultaneously observe the various production reactions and events caused by hypernuclei. We have already observed several events with hypernuclear fragments associated with sequential decay and scattering with nuclei in the emulsion sheet. Further developments with machine learning and nuclear emulsion techniques promote experimental studies of hypernuclei.

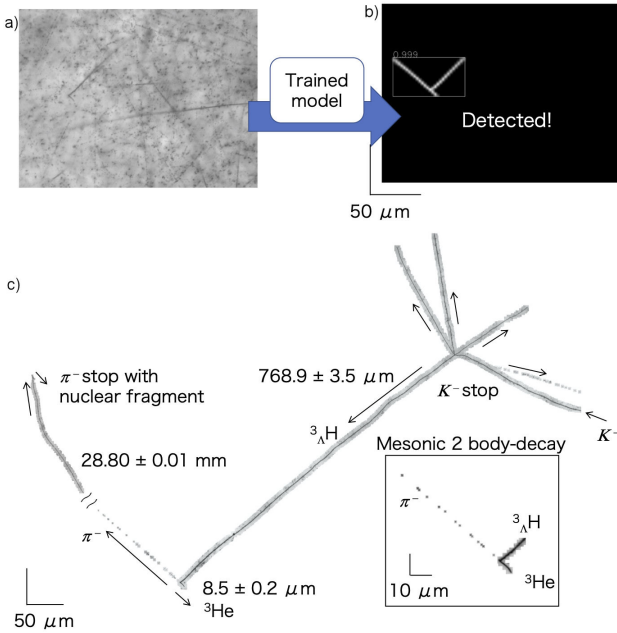


FIGURE 3. Detection of hypertriton events by the developed object detection model. Panels a) and b) show the microscope image of emulsion and the mask information corresponding to the position and topology of the two-body decay of the hypertriton detected by the model, respectively. Panel c) shows the overall view of the first hypertriton event detected in the emulsion of the E07 experiment. The stopped event with the fragmentation of the π^- and production point of hypertriton were also observed [18].

1. M. Danysz & J. Pniewski Delayed disintegration of a heavy nuclear fragment *I. Phil. Mag.* **44** (1953) 348, <https://doi.org/10.1080/14786440308520318>
2. G. Bohm et al. A determination of the binding-energy values of light hypernuclei. *Nucl. Phys. B* **4** (1968) 511, [https://doi.org/10.1016/0550-3213\(68\)90109-0](https://doi.org/10.1016/0550-3213(68)90109-0)
3. M. Juric et al. A new determination of the binding-energy values of the light hypernuclei ($A \leq 15$). *Nucl. Phys. B* **52** (1973) 1, [https://doi.org/10.1016/0550-3213\(73\)90084-9](https://doi.org/10.1016/0550-3213(73)90084-9)
4. O. Hashimoto, H. Tamura Spectroscopy of hypernuclei. *Prog. Part. Nucl. Phys.* **57** (2006) 564, <https://doi.org/10.1016/j.pnpnp.2005.07.001>
5. O. Hashimoto, et al. Hypernuclear Spectroscopy at JLab Hall C. *Nucl. Phys. A* **835** (2010) 121, <https://doi.org/10.1016/j.nuclphysa.2010.01.184>
6. C. Rappold et al. J. Phys. Overview of the hypernuclear production in heavy-ion collision experiments *Conf. Ser.* **668** (2016) 012025, <https://doi.org/10.1088/1742-6596/668/1/012025>
7. Particle Data Group et al. Review of particle physics. *Prog. Theor. Exp. Phys.* **2020** (2020) 083C01, <https://doi.org/10.1093/ptep/ptaa104>
8. C. Rappold et al. Hypernuclear spectroscopy of products from 6Li projectiles on a carbon target at 2 AGeV. *Nucl. Phys. A* **913** (2013) 170, <https://doi.org/10.1016/j.nuclphysa.2013.05.019>
9. The STAR Collaboration. Observation of an antimatter hypernucleus. *Science* **328** (2010) 58, <https://www.science.org/doi/10.1126/science.1183980>
10. J. Adam et al. ${}^3_{\Lambda}\text{H}$ and ${}^3_{\Lambda}\bar{\text{H}}$ production in Pb-Pb collisions at $\sqrt{s_{NN}} = 2.76$ TeV. *Phys. Lett. B* **754** (2016) 360,
11. L. Adamczyk et al. Measurement of the ${}^3_{\Lambda}\text{H}$ lifetime in Au+Au collisions at the BNL Relativistic Heavy Ion Collider. *Phys. Rev. C* **97** (2018) 054909, <https://doi.org/10.1103/PhysRevC.97.054909>
12. J. Chen, D. Keane, Y.-G. Ma, A. Tang, & Z. Xu. Antinuclei in heavy-ion collisions. *Phys. Rep.* **760** (2018) 1, <https://doi.org/10.1016/j.physrep.2018.07.002>
13. S. Acharya et al. ${}^3_{\Lambda}\text{H}$ and ${}^3_{\Lambda}\bar{\text{H}}$ lifetime measurement in Pb-Pb collisions at $\sqrt{s_{NN}} = 5.02$ TeV via two-body decay. *Phys. Lett. B* **797** (2019) 134905, <https://doi.org/10.1016/j.physletb.2019.134905>
14. A. Perez-Obiol, D. Gazda, E. Friedman & A. Gal. Revisiting the hypertriton lifetime puzzle. *Phys. Lett. B* **811** (2020) 135916, <https://doi.org/10.1016/j.physletb.2020.135916>
15. J. Adam et al. Measurement of the mass difference and the binding energy of the hypertriton and antihypertriton. *Nat. Phys.* **16** (2020) 409, <https://doi.org/10.1038/s41567-020-0799-7>
16. Y-H .Leung et.al. Hypernuclei and anti-hypernuclei production in heavy-ion collisions. <https://indico.cern.ch/event/985652/contributions/4296086/attachments/2248875/3814733/sqm2021hypernucleiv7.pdf>
17. Y. Toyama, et al., Status of a Lifetime Measurement of Light Hypernuclei Using High Intensity Tagged Photon Beam at ELPH. Proceedings of the 8th International Conference on Quarks and Nuclear Physics (QNP2018) (2019). DOI10.7566/jpscp.26.031018
18. T.R Saito et al., New directions in hypernuclear physics. *Nature Reviews Physics* (2021) 2522, 10.1038/s42254-021-00371-w
19. H. Asano et al., ${}^3_{\Lambda}\text{H}$ and ${}^4_{\Lambda}\text{H}$ mesonic weak decay lifetime measurement with ${}^{3,4}\text{He}(K^-, \pi^0){}^3,4_{\Lambda}\text{H}$ reaction. http://j-parc.jp/researcher/Hadron/en/pac_1901/pdf/P73.2019-06.pdf
20. M. Agnello et al., Direct measurement of the ${}^3_{\Lambda}\text{H}$ and ${}^4_{\Lambda}\text{H}$ lifetimes using the ${}^{3,4}\text{He}(\pi^-, K^0){}^3,4_{\Lambda}\text{H}$ reactions. http://j-parc.jp/researcher/Hadron/en/pac_1901/pdf/P74.2019-08.pdf
21. D. Cebra, Beam Energy Scan II (BES-II) and FXT: Status and Plans https://indico.gsi.de/event/5593/contributions/25859/attachments/18918/23737/CBM-STAR_Workshop_Mar2017_Cebra.pdf
22. M. FaseUpgrade of the ALICE experiment for LHC Run 3 and beyond <https://indico.bnl.gov/event/9726/contributions/46030/attachments/33844/54487/upgradeALICE.pdf>
23. K Imai, K. Nakazawa, & H. Tamura. J-PARC E07 experiment: Systematic study of double strangeness system with an emulsion-counter hybrid method. Proposal for Nuclear and Particle Physics Experiments at J-PARC. (2006) http://j-parc.jp/researcher/Hadron/en/pac_0606/pdf/p07-Nakazawa.pdf
24. M.K. Soe et al. Automatic track following system to study double strangeness nuclei in nuclear emulsion exposed to the observable limit. *Nucl. Instrum. Methods Phys. Res. A* **848** (2017) 66, <https://doi.org/10.1016/j.nima.2016.12.046>
25. H. Ekawa et al. Observation of a Be double-Lambda hypernucleus in the J-PARC E07 experiment. *Prog. Theor. Exp. Phys.* **2019** (2019) 021D02, <https://doi.org/10.1093/ptep/pty149>
26. S. H. Hayakawa et al. Observation of coulomb-assisted nuclear bound state of $\Xi^{-}{}^{14}\text{N}$ system. *Phys. Rev. Lett.* **126** (2021) 062501, <https://doi.org/10.1103/PhysRevLett.126.062501>
27. M. Yoshimoto et al. First observation of a nuclear s-state of a Ξ hypernucleus, ${}^{15}_{\Xi}\text{C}$. *Prog. Theor. Exp. Phys.* **2021** (2021) 073D02, <https://doi.org/10.1093/ptep/ptab073>
28. K. Nakazawa et al. The first evidence of a deeply bound state of Ξ^{-} - ${}^{14}\text{N}$ system. *Prog. Theor. Exp. Phys.* **3** (2015) 033D02 (2015) <https://doi.org/10.1093/ptep/ptv008>
29. J. Yoshida et al. A new scanning system for alpha decay events as calibration sources for range-energy relation in nuclear emulsion. *Nucl. Instrum. Methods Phys. Res. A* **847** (2017)

- 86, <https://doi.org/10.1016/j.nima.2016.11.044>
30. Y. LeCun, Y. Bengio & G. Hinton. Deep learning. *Nature* **521** (2015) 436, <https://doi.org/10.1038/nature14539>
31. K. He, X. Zhang, S. Ren & J. Sun. Deep residual learning for image recognition. Preprint at arXiv (2015). <http://arxiv.org/abs/1512.03385>
32. J. Yoshida *et al.* CNN-based event classification of alpha-decay events in nuclear emulsion. *Nucl. Instrum. Methods Phys. Res. A* **989**, (2021) 164930, <https://doi.org/10.1016/j.nima.2020.164930>
33. K. He, G. Gkioxari, P. Dollar, & R. B. Girshick. Mask R-CNN. Preprint at arXiv (2017). <https://arxiv.org/abs/1703.06870>
34. J. Allison *et al.*, Recent developments in Geant4. *Nucl. Instrum. Methods Phys. Res. A* **835** 186-225. (2016) <https://www.sciencedirect.com/science/article/pii/S0168900216306957>
35. T. Wang *et al.*, High-resolution image synthesis and semantic manipulation with conditional GANs. Preprint at arXiv <http://arxiv.org/abs/1711.11585> (2017).
36. I. J. Goodfellow *et al.*, Generative adversarial networks. Preprint at arXiv <https://arxiv.org/abs/1406.2661> (2014)
37. W.H Barkas. Nuclear Research Emulsions. Pure & Applied Physics Series 15-1 (Academic, 1963).
38. E. Liu *et al.*, Revisiting the former nuclear emulsion data for hypertriton. *Eur. Phys. J. A* **57** (2021) 327, <https://doi.org/10.1140/epja/s10050-021-00649-8>
39. A. Esser *et al.*, Observation of ${}^4_{\Lambda}$ H Hyperhydrogen by Decay-Pion Spectroscopy in Electron Scattering. *Phys. Rev. Lett* **114** (2015) 232501, <https://link.aps.org/doi/10.1103/PhysRevLett.114.232501>